The authors express their gratitude to Mrs J. Jelínková for preparing Figs. 1 and 2.

References

BUERGER, M. J. (1957). *Z. Kristallogr.* **109**, 42-60.
EISENSTEIN, G. (1851). *J. Math. Crelle*, **41**, 141-190.
GRUBER, B. (1973). *Acta Cryst.* A**29**, 433-440.
GRUBER, B. (1980). Private communication.
GRUBER, B. (1989). *Acta Cryst.* A**45**, 123-131.
International Tables for Crystallography (1987). Vol. A, 2nd. ed. Ch. 9.3, especially Table 9.3.1. Dordrecht: Kluwer.
MIGHELL, A. D. & RODGERS, J. R. (1969). *International Tables for X-ray Crystallography*, Vol. I, 3rd ed., pp. 530-535. Birmingham: Kynoch Press.
NIGGLI, P. (1928). *Handbuch der Experimentalphysik*, Vol. 7, Part 1, pp. 108-176. Leipzig: Akademische Verlagsgesellschaft.
WOLFF, P. M. DE (1988). *Comput. Math. Appl.* **16**, 487-492.

Acta Cryst. (1991). A**47**, 36-39

Determination of the Sign of a Dislocation in a ZnTe Crystal by Convergent-Beam Electron Diffraction*

BY F. NIU, R. WANG AND G. LU

Department of Physics, Wuhan University, 430072 *Wuhan, People's Republic of China*

(*Received* 22 *May* 1990; *accepted* 29 *August* 1990)

Abstract

The twist and distortion of diffraction fringes in a convergent-beam electron diffraction pattern, caused by a dislocation in a ZnTe crystal, have been studied systematically. It has been found that the sense of such a twist reverses when the beam crossover changes from one side of the specimen to the other. From a qualitative consideration, it has been concluded that the diffraction fringes on the side pointed to by the vector $\mathbf{u}\times\mathbf{c}$ are shifted along $\mathbf{b}$. This phenomenon can be used to determine the sign of the Burgers vector of a dislocation.

1. Introduction

Recently, progress has been made in studying dislocations in crystals by means of convergent-beam electron diffraction (CBED). After the initial work of Carpenter & Spence (1982), it was proposed that diffraction fringes in the central disc may be used to determine the Burgers vector of a dislocation (Cherns & Preston, 1986; Cherns, Kiely & Preston, 1988; Tanaka, Terauchi & Kaneyama, 1988). Wen, Wang & Lu (1989) noticed that the zeroth-order Laue-zone (ZOLZ) pattern in the central disc is convenient for studying the geometry of dislocations, and they made extensive computer simulations to verify its feasibility in various dislocation cases (Lu, Wen, Zhang & Wang, 1990). These authors also pointed out that the position of the convergent-beam crossover relative to the specimen can greatly influence the ZOLZ pattern, and thus it is important in determining the sign of the Burgers vector of a dislocation. In this paper, we report the investigation of the influence of dislocations in a II-VI semiconductor compound ZnTe crystal on diffraction fringes in the central discs in defocused CBED patterns. We make clear that both the value and the sign of Δf can influence the detail characteristics of the distorted diffraction fringes.

2. Experiments

A ZnTe polycrystal was compressed along the crystal growing axis. The compressed crystal was sliced with a wire saw to about 200 μm, and the surface normal of the slices is about 45° from the growing axis. The deformed ZnTe was ground and polished mechanically down to about 40 μm. The specimens were then ion-beam thinned for the observation of transmission electron microscopy (TEM).

The CBED experiments were carried out on a JEM-100CX(II) transmission electron microscope by lowering the specimen stage. The beam crossover can be moved above or below the specimen a distance Δf by changing the objective-lens current with the FOCUS knob. Then the condenser-lens current is adjusted to form a pattern consisting of sharp spots under the imaging mode. Each spot in this pattern corresponds to an image (bright-field image or dark-field image). The defocus value Δf is measured using the distance R of a dark-field image from the bright-field image (the center spot): $\Delta f = R/(2\theta_B)$ with θ_B being the Bragg angle of this dark-field spot. In this paper, the positive sense of Δf is taken downwards from the specimen along the optical axis. Owing to a defocus illumination, the shadow image of a dislocation and the distortion of diffraction fringes can be observed simultaneously.

* Project supported by the National Natural Science Foundation of China.

0108-7673/91/010036-04$03.00

3. Results

Fig. 1(*a*) is a CBED pattern taken from a perfect region. The diffraction fringes are indexed with the help of the computer simulation program which was developed by Jiao, Zou & Wang (1987), see Fig. 1(*b*). Figs. 1(*c*) and (*d*) are respectively underfocused ($\Delta f<0$) and overfocused ($\Delta f>0$) CBED patterns from the same dislocation, of which the shadow image is indicated by arrows in Fig. 1(*c*). They have approximately the same defocus values but opposite signs. When crossing the dislocation, the diffraction fringes, *e.g.* $4\bar{4}0$ and $\bar{4}80$, are seen to be split and twisted, and they are shifted toward the opposite directions on the opposite sides of the dislocation shadow image. Furthermore, the sense of such a twist reverses when the beam crossover changes from one side of the specimen to the other.

Not only the sign but also the magnitude of Δf can influence the distortion of the diffraction fringes when a dislocation is in the beam path. When $|\Delta f|$ is large enough, the splitting of the diffraction fringe caused by the displacement field of the dislocation cannot be resolved and only a twisting behavior is observed.

4. Discussion

The strain field **R** of a dislocation acts like a local rotation of the Bragg planes and changes the effective deviation parameter s to $s'=s+\beta'_g=s+\mathbf{g}\,.\,\mathrm{d}R/\mathrm{d}z$ (Hirsch, Howie, Nicholson, Pashley & Whelan, 1977). It should be noticed that β'_g changes its sense when going from one side of a dislocation to the other side, if the contribution of the term $\mathbf{g}\,.\,\mathbf{b}\times\mathbf{u}$ is negligible (Hirsch, Howie, Nicholson, Pashley & Whelan, 1977).

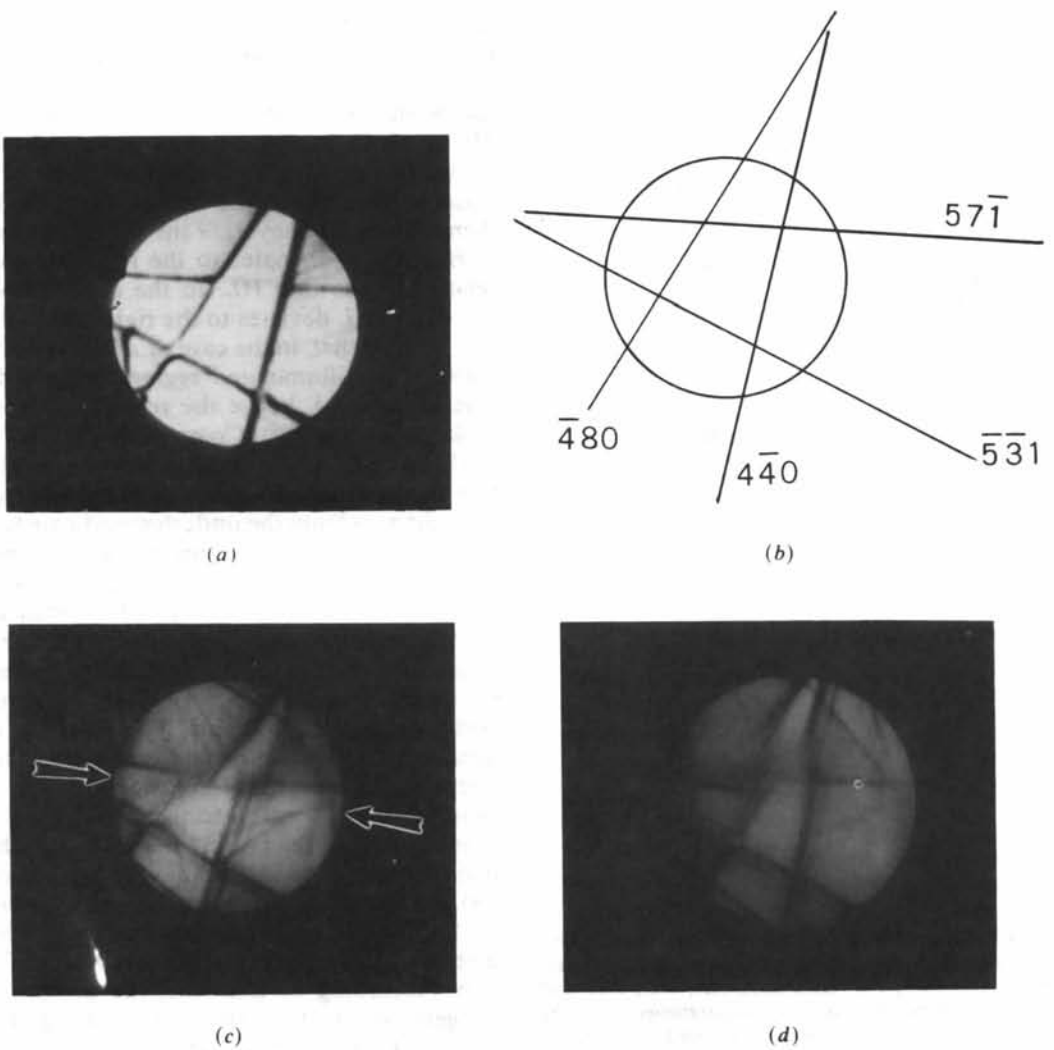

Fig. 1. Central discs of CBED patterns at 100 kV from a ZnTe crystal. (*a*) From a perfect region. (*b*) Simulated pattern. (*c*) $\Delta f=-8$ μm. (*d*) $\Delta f=8$ μm. (*c*) and (*d*) are from a region containing a dislocation line of which the shadow image is indicated by arrows.

When the beam crossover is above the specimen ($\Delta f<0$, underfocused) as shown in Fig. 2(a), the formation of a distorted diffraction fringe in a CBED pattern is shown in Figs. 2(b) and (c). Fig. 2(b) illustrates a region on the surface of a perfect specimen illuminated by the electron beam. Line HL corresponds to the region where Bragg condition $s=0$ is satisfied. Vector $\mathbf{g}_p$ (the projection of $\mathbf{g}$) and the line HL are perpendicular to the electron beam. In Fig. 2(a), it is readily seen that the area with $s<0$ is the area which is pointed to by $\mathbf{g}_p$. Fig. 2(c) shows the region, illuminated by the convergent-beam electron beam, which contains a left-hand screw dislocation line DS with its Burgers vector $\mathbf{b}$ and line vector $\mathbf{u}$ as shown in the figure. In the present paper, the FS/RH (perfect crystal) convention (Hirsch *et al.*, 1977) is used. The dashed line HL still shows the region where $s=0$ is satisfied for a perfect crystal. Nonetheless, near the dislocation, this region should be replaced by the region where $s'=s+\beta'_g=0$ is satisfied as discussed above. In the case shown in Fig. 2(c), the region in which $\beta'_g>0$ lies above DS, then the line that satisfies $s'=0$ is HH' which deviates towards the area with $s<0$, *i.e.* to the right-hand side of HL. For the area below DS, the opposite deviation occurs, *i.e.* the $s'=0$ line $L'L$ is deviated to the left-hand side ($s>0$). Fig. 2(c) can also be seen as the real defocus CBED pattern that can be observed on the screen. DS stands for the shadow image of a dislocation and HH' and $L'L$ stand for the two halves of a diffraction fringe.

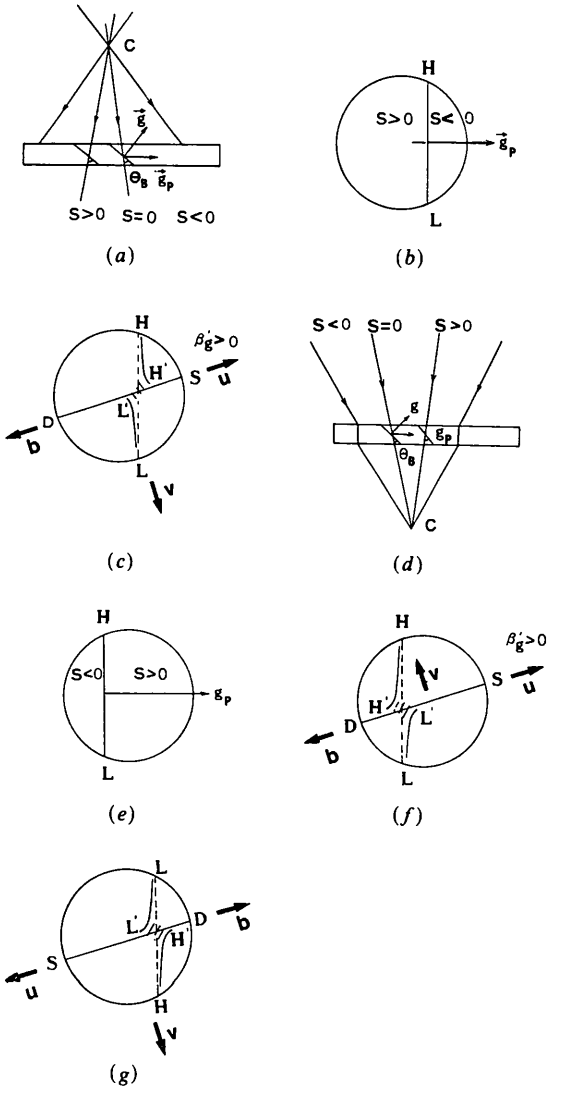

Fig. 2. Schematic illustration showing the formation of a distorted diffraction fringe and its dependence on the position of the beam crossover. C: crossover; DS: dislocation line; HL', HH' and LL': regions in which the effective deviation parameter $s'=s+\beta'_g$ is equal to zero. (a), (b), (c) $\Delta f<0$, underfocused; (d), (e), (f) and (g) $\Delta f>0$, overfocused; (b) and (e) perfect-specimen regions; (c) and (f) specimen regions with dislocation line DS; (c) and (g) central discs of the CBED patterns.

When the beam crossover is below the specimen ($\Delta f>0$, overfocused) as is the case in Fig. 2(d), the formation of a distorted diffraction fringe in a CBED pattern is shown in Figs. 2(e), (f) and (g). The specimen region on the right-hand side of the line HL to which $\mathbf{g}_p$ points now corresponds to $s>0$ as shown in Fig. 2(e) for the perfect crystal. When there exists a dislocation line DS as shown in Fig. 2(f), then in the area above DS the region satisfying $s'=0$ is HH' which deviates to the left-hand side ($s<0$) relative to the line HL. In the area below DS, the $s'=0$ line $L'L$ deviates to the right-hand side ($s>0$). It is noticed that, in the case of $\Delta f>0$, a 180° rotation between the illuminated region and the diffraction disc is involved, hence the real CBED central disc looks as in Fig. 2(g). Comparing Fig. 2(c) with Fig. 2(g), we find that the sense of the twist of the diffraction fringe is indeed reversed when the beam crossover changes from the underfocused case to the overfocused case. This argument thus explains the observed distortion of diffraction fringes and their dependence on the position of the beam crossover.

A vector $\mathbf{v}=\mathbf{u}\times\mathbf{c}$ was introduced to define the sense of the distortion of ZOLZ patterns caused by a dislocation by Wen, Wang & Lu (1989) where $\mathbf{c}$ is the vector pointing to the beam crossover from a dislocation line and $\mathbf{u}$ is the direction vector of the dislocation line. This vector is also found useful in the distortion of a general diffraction fringe crossing a dislocation as in the case of the present work. That is, the diffraction fringes on the side pointed to by the vector $\mathbf{v}$ (or $-\mathbf{v}$) are shifted along $\mathbf{b}$ (or $-\mathbf{b}$), as shown in Figs. 2(c), (f) and (g). This phenomenon can be used to determine the sense of the Burgers vector of a dislocation. According to this rule, the projection of the Burgers vector of the dislocation in Fig. 1 is almost pointing to the left-hand side, when the line direction is selected to be pointing to the right-hand side. This means that this dislocation possesses a left-hand

screw component. By using the method for determining the Burgers vector proposed by Tanaka, Terauchi & Kaneyama (1988), the Burgers vector is determined to be $\frac{1}{2}[011]$ or $\frac{1}{2}[01\bar{1}]$.

References

CARPENTER, R. W. & SPENCE, J. C. H. (1982). *Acta Cryst.* A**38**, 55-61.

CHERNS, D., KIELY, C. J. & PRESTON, A. R. (1988). *Ultramicroscopy*, **24**, 355-369.

CHERNS, D. & PRESTON, A. R. (1986). Proc. XIth Int. Congr. on Electron Microscopy, Kyoto, Japan, pp. 721-722.

HIRSCH, P., HOWIE, A., NICHOLSON, R. B., PASHLEY, D. W. & WHELAN, M. J. (1977). *Electron Microscopy of Thin Crystals*, pp. 164, 178, 198, 250. Huntington, New York: Robert E. Krieger.

JIAO, S., ZOU, H. & WANG, R. (1987). *J. Chin. Electron Microsc. Soc.* **6**, 42-47. (In Chinese.)

LU, G., WEN, J. G., ZHANG, W. & WANG, R. (1990). *Acta Cryst.* A**46**, 103-112.

TANAKA, M., TERAUCHI, M. & KANEYAMA, T. (1988). *Convergent-Beam Electron Diffraction* II, pp. 160-185. Tokyo: JEOL-Maruzen.

WEN, J., WANG, R. & LU, G. (1989). *Acta Cryst.* A**45**, 422-427.

Acta Cryst. (1991). A**47**, 39-44

Effects of Crystal-Surface Inclination on X-ray Multiple Diffraction: Intensity Variation and Phase Determination

BY KUANG-CHIH LEE AND SHIH-LIN CHANG

Department of Physics, National Tsing Hua University, Hsinchu, Taiwan 30043

(*Received* 21 *July* 1989; *accepted* 3 *September* 1990)

Abstract

Effects of crystal-surface inclination on the intensities of X-ray *Umweganregung* multiple diffractions are investigated for perfect silicon crystals. The intensity variations of the multiply diffracted beams due to the surface inclination are accounted for in terms of three-beam dynamical calculations. Quantitative phase determination direct from the intensity profile analysis is also carried out. It is found that the phase determination is not affected by the crystal-surface inclination. This conclusion is also supported by the analysis of the profile asymmetry.

1. Introduction

X-ray multiple diffraction takes place when several sets of atomic planes are simultaneously brought into position to diffract an incident X-ray beam. The coherent dynamical interaction among the multiply diffracted waves, which governs the diffraction intensities, has long been investigated for Borrmann (transmission) geometry (Borrmann & Hartwig, 1965; Saccocio & Zajac, 1965; Hildebrandt, 1967; Joko & Fukuhara, 1967; Ewald & Heno, 1968; Uebach & Hildebrandt, 1969; Balter, Feldman & Post, 1971; Umeno & Hildebrandt, 1975; Post, Chang & Huang, 1977; Høier & Aanestad, 1981; Campos & Chang, 1986; and many others), and for Renninger (reflection) geometry (Renninger, 1937; Colella, 1974; Chapman, Yoder & Colella, 1981; Chang, 1981, 1982; Juretschke, 1982*a*, *b*; Hümmer & Billy, 1982, 1986; Post, 1983; Post, Nicolosi & Ladell, 1984; Shen, 1986; Thorkildsen, 1987; Chang & Tang, 1988; and many others). Besides, the extraction of phase information from the intensity distribution of multiple diffractions has recently become one of the major themes in this particular area of research. Reports on this subject include articles by Hart & Lang (1961), Ewald & Heno (1968), Colella (1974), Post (1977), Jagodzinski (1980), Chapman, Yoder & Colella (1981), Chang (1981, 1982), Høier & Aanestad (1981), Juretschke (1982*a*), Hümmer & Billy (1982), Post (1983), Post, Nicolosi & Ladell (1984), Shen (1986) and Mo, Haubach & Thorkildsen (1988) for centrosymmetric crystals, and by Juretschke (1982*b*), Chang & Valladares (1985), Hümmer & Billy (1986), Shen & Colella (1988), Tang & Chang (1988) and Hümmer, Weckert & Bondza (1989) for noncentrosymmetric crystals.

Very recently, a quantitative phase-determination procedure using three-beam diffraction-intensity profiles has been proposed (Chang & Tang, 1988). Experimental phase determination has also been realized for perfect-crystal plates (Tang & Chang, 1988). In that approach, the intensity due to dynamical interaction, which may be separated from the total intensity distribution, is directly related to the phases of the involved structure-factor multiplets. As far as the dynamical effect in multibeam diffraction is concerned, the excitation of the dispersion surface governed by the crystal boundary plays a key role in the allocation of the total energy into the diffracted waves. Namely, the diffraction intensities depend also on the crystal boundary. Recently, Kov'ev & Deigen (1987) have reported the intensity variation over

0108-7673/91/010039-06$03.00